differ significantly from the femoral epiphyses of extant juvenile crocodilians and precocial birds when the latter are prepared by bacterial maceration to remove the articular cartilage cap (Fig. 3). Thus, long bones of *Maiasaura* probably originally had a typical archosaurian articular fibrocartilaginous cap. In life, this dinosaur's long bones were probably similar to those of all extant archosaurians, whether altricial or precocial. Moreover, the femoral growth plate of perinatal *Maiasaura* is similar to that of a 2-week-old chicken (*Gallus*), a thoroughly precocial taxon (*8*).

Embryonic femora of the hypsilophodont ornithopod *Orodromeus* (Archosauria: Ornithischia) were described as having "well formed, smooth condyles which, although fully ossified in appearance, are formed entirely of calcified cartilage. Endochondral bone is not observed in the epiphyseal or metaphyseal regions" (*1*, p. 256). This description is problematic insofar as in extant, perinatal archosaurians, whether altricial or precocial, articular condyles of the long bones are not composed of calcified cartilage. Calcified cartilage forms in the deepest layer of the growth zone, where it is a scaffold for the deposition of new endochondral bone. Without the association between calcified cartilage and endochondral bone, there is no capacity for long bone elongation. Consequently, we suggest that interpretation of perinatal long bone structure in *Orodromeus* deserves reexamination.

Data from extant specimens indicate that there are no qualitative differences in the development of long bone epiphyseal structure in archosaurians, whether altricial or precocial. It has also been suggested that the lack of well-formed processes for muscle attachment (for example, trochanteric processes) in neonatal *Maiasaura* may be indicative of its altricial nature (*1*). However, well-formed processes did not exist in any of our precocial or altricial neonatal specimens. These processes apparently form much later in response to muscle-induced mechanical stresses on the long bones.

It has also been hypothesized that contemporaneous preservation of juvenile and adult *Maiasaura* in or near presumed colonial nesting sites somehow indicates that neonates were altricial and that the young were completely dependent on adult care. However, this evidence is equivocal: parents and juvenile crocodilians, as well as some precocial birds [for example, many shorebirds (Charadriiformes)], often remain in or near colonial nesting sites for some time after hatching (*9*, *10*).

Similarly, the discovery of eggs in close association with an adult *Oviraptor* has been interpreted as evidence of birdlike parental behavior, including perhaps endothermy and incubation of eggs by adults (*11*). However, nest-attending and brooding behavior is widely distributed among extant crocodilians, lizards, snakes, and amphibians (*12–15*). For example, female crocodiles (*Crocodilus niloticus*) often rest their lower throat or thorax directly on the nest for the duration of the 90-day incubation period (*16*). Speculation regarding parental incubation of eggs and endothermy based on the apparent brooding behavior of *Oviraptor* are, at best, tenuous. Current evidence suggests that the nesting behavior of dinosaurs was likely similar to that of modern crocodilians.

REFERENCES AND NOTES

1. J. R. Horner and D. B. Weishampel, *Nature* **332**, 256 (1988).
2. J. M. Starck, *J. Morphol.* **222**, 113 (1994); *Zeitmuster der Ontogenesen bei Nestflüchtenden und Nesthockenden Vögeln (Courier Forschungsinstitut Senckenberg*, Herausgegeben von der Senckenbergischen Naturforschenden Gesellschaft, Frankfurt, 1989), vol. 114.
3. J. R. Horner and P. J. Currie, in *Dinosaur Eggs and Babies*, K. Carpenter, K. F. Hirsch, J. R. Horner, Eds. (Cambridge Univ. Press, New York, 1994), p. 312.
4. M. A. Norell, personal communication.
5. P. Currie, personal communication.
6. D. B. Weishampel and J. R. Horner, in *Dinosaur Eggs and Babies*, K. Carpenter, K. F. Hirsch, J. R. Horner, Eds. (Cambridge Univ. Press, New York, 1994), p. 229.
7. R. W. Haines, in *Biology of the Reptilia*, C. Gans, A. d'A. Bellairs, T. S. Parsons, Eds. (Academic Press, London, 1969), vol. 1, p. 81.
8. C. Barreto, R. M. Albrecht, D. E. Bjorling, J. R. Horner, N. J. Wilsman, *Science* **262**, 2020 (1993).
9. J. W. Lang, in *Crocodiles and Alligators*, C. A. Ross, Ed. (Facts On File, New York, 1989), p. 102.
10. F. B. Gill, *Ornithology* (Freeman, New York, 1990).
11. M. A. Norell, J. M. Clark, L. M. Chiappe, D. Dashzeveg, *Nature* **378**, 774 (1995).
12. W. E. Magnusson, K. A. Vliet, A. C. Pooley, R. Whitaker, in *Crocodiles and Alligators*, C. A. Ross, Ed. (Facts On File, New York, 1989), p. 118.
13. G. K. Noble and E. R. Mason, *Am. Mus. Novit.* **619**, 1 (1933).
14. S. A. Minton, in *The Encyclopedia of Reptiles and Amphibians*, T. Halliday and K. Adler, Eds. (Facts On File, New York, 1987), p. 112.
15. W. E. Duellman and L. Trueb, *Biology of Amphibians* (Johns Hopkins Univ. Press, Baltimore, MD, 1986), p. 13.
16. H. B. Cott, *Trans. Zool. Soc. London* **29**, 211 (1961).

17. We thank J. Aikin for eagle radiographs; D. Belcher for advice; A. Boehmer for translations; R. Elsie for donation of hatchling alligators; J. Horner for allowing us access to fossil specimens; J. Hillenius for review and photography; T. Hovie for photography; J. Matoon, K. Timm, and B. Watrous for radiographic assistance; R. Pickton for bird specimens; M. Schadt for histological preparations; F. C. Sibley for loan of megapode specimens; G. Smith and N. Smith for donation of emu specimens; B. Taylor for photomicroscopy advice; and G. Vaillancourt and D. Vaillancourt for donation of ostrich specimens. We thank J. Ruben for support and comments. Supported by funds from the Oregon State University Department of Zoology and NSF grant IBN-9420290 to W. J. Hillenius and J. A. Ruben.

23 January 1996; accepted 6 March 1996

Concentrations of Tropospheric Ozone from 1979 to 1992 over Tropical Pacific South America from TOMS Data

Yibo Jiang and Yuk L. Yung*

An estimate of tropospheric ozone concentrations was obtained from the difference in the Total Ozone Mapping Spectrometer (TOMS) data between the high Andes and the Pacific Ocean. From 1979 to 1992 the tropospheric ozone concentration apparently increased by 1.48 ± 0.40 percent per year or 0.21 ± 0.06 Dobson unit per year over South America and the surrounding oceans. An increase in biomass burning in the Southern Hemisphere can account for this trend in tropospheric ozone concentrations.

Tropospheric O_3 plays a key role in regulating the chemical composition and climate of the troposphere (*1*). The photolysis of O_3 forms $O(^1D)$, which reacts with H_2O to form reactive HO_x radicals in the troposphere. These radicals in turn undergo a series of chemical reactions that are important for the lifetimes of a large number of gases (for example, CH_4, CO, and CH_3X, where X is a halogen or nitrile). Moreover, O_3 is associated with air pollution. Its increase in the atmosphere is of concern because of its deleterious effects on vegetation and human health.

There is general agreement that tropospheric O_3 concentrations have increased in recent decades in the temperate zones in the Northern Hemisphere, but trends seem to vary geographically and temporally. A regional increase in tropospheric O_3 concentrations was first documented by Warmbt (*2*), who analyzed a 20-year record of surface O_3 measurements at stations in Germany between the mid-1950s and 1970s. Analyses of the vertical dependence of the O_3 concentrations were then attempted, based on the record of ozonesonde readings (*3–6*). These studies typically showed an increase in O_3 concentrations of about 1% per year in the lower troposphere.

Division of Geological and Planetary Sciences, California Institute of Technology, Pasadena, CA 91125, USA.

*To whom correspondence should be addressed.

However, detailed analysis revealed that from 1979 to 1982 the O_3 concentrations in the layer from 0 to 5 km varied from year to year by −2 to 3% per year among 12 ozonesonde stations at mid- and high-latitudes in the Northern Hemisphere (*5*). Recently, Tarasick *et al.* (*7*) found that tropospheric O_3 concentrations had decreased over Canada from 1980 to 1993. On the other hand, there have been few measurements in the Southern Hemisphere. In this study, we used space-borne measurements of tropospheric O_3 to show that tropospheric O_3 concentrations have increased over Pacific South America from 1979 to 1992.

The Total Ozone Mapping Spectrometer (TOMS) instrument on the Nimbus 7 spacecraft was used to measure the spatial distribution of total O_3 from 1978 until 6 May 1993. By scanning across the track of the satellite, TOMS obtained data between successive satellite orbital tracks. We used the daily TOMS gridded O_3 data of Version 7 (*8*) (on a 1° by 1.25° grid in latitude and longitude) from 1979 to 1992. The improvements of Version 7 over Version 6 that are essential for this work are as follows: (i) improved International Satellite Cloud Climatology Project (ISCCP) cloud height climatology and higher resolution terrain height maps, (ii) use of a more accurate model for partially clouded scenes, and (iii) improved radiative transfer calculations for table generation. The most important improvement for this work is the removal of the overestimate of the total O_3 due to the low marine stratus clouds.

The high Andes along the west coast of central South America and the nearby ocean provides a topographic contrast in which the TOMS data can be used to examine O_3 concentrations in the lower troposphere by difference. The highest mountain in Peru is 6768 m above sea level, and the highest mountain in Chile is 6908 m above sea level. Therefore, the total column O_3 measurement by TOMS in these regions will be above the bulk of the troposphere. For a region spanning only a few degrees in latitude and longitude, we assume that the vertical distribution of O_3 does not change (*9*). Taking the January 1980 column O_3 map as an example (Fig. 1), the column O_3 is relatively smooth in the east-west direction over South America, except for the region near the Andes, where O_3 concentrations are low. Because TOMS measured column O_3 from the top of the atmosphere to the surface of Earth, the difference in the TOMS column O_3 from the mountains to the surrounding ocean gives the column O_3 value from sea level to the top of the mountains about 6 km above sea level.

To examine trends in this difference, we analyzed monthly mean TOMS column O_3 values averaged over a selected 24 points over the Andes and the oceans (Fig. 1) (*10*). From 1979 to 1992, the ocean (higher) O_3 showed no obvious trend (Fig. 2A), which is consistent with results in the equatorial region (*11*). However, the difference, the tropospheric column O_3 in the layer from 0 to 6 km (Fig. 2B) (*12*), has increased by about 1.48 ± 0.40% per year relative to the reference tropospheric column O_3 of 14.34 DU in 1979, which is consistent with the trend obtained through the use of the tropospheric residual technique (*13, 14*). This value is equivalent to an increase of 0.21 ± 0.06 DU per year. The years with El Niño events (1982–1983 and 1986–1987) are marked by lower O_3 values.

Some comparison of these results is possible if we use the ozonesonde measurements taken nearby at Natal, Brazil (6°S, 35°W) (*15, 16*). Data have been obtained here from 1978 to 1988; however, these data are relatively sparse and the times of the O_3 soundings are unevenly distributed (*16*) and are not adequate to study O_3 trends, although they can be used to assess our tropospheric column O_3 calculation. Our estimate shows an O_3 column of 20.29 DU in the layer from 0 to 6 km in September 1987 as compared with about 16.33 DU at Natal. In addition, both data sets show high concentrations of O_3 from August to November in each year. Considering the roughness in the calculation of column O_3 at Natal, the two data sets agree.

A likely cause of the increase in O_3 concentrations is an increase in biomass burning (*13, 14*). As shown in Fig. 3A, which plots the rate of the biomass burning (*17*) from 20° to 30°S, the seasonality of the tropospheric O_3 is well correlated with the seasonality of the rate of biomass burning. Both O_3 column amounts and rates of biomass burning were high from August to November in each year. Although it is hard to separate the stratospheric sources from anthropogenic sources of tropospheric O_3, this result suggests that the higher values of O_3 between August and November are the direct consequences of biomass burning. The anomalous low O_3 concentration in El

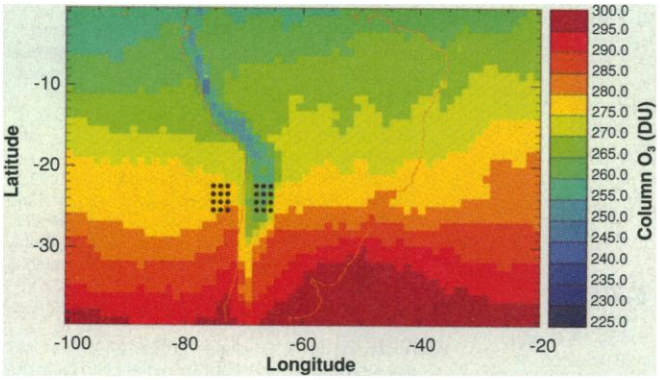

Fig. 1. Monthly averaged column O_3 for January 1980 from TOMS. The black dots are the 24 points used in the analysis. The TOMS data are from (*8*).

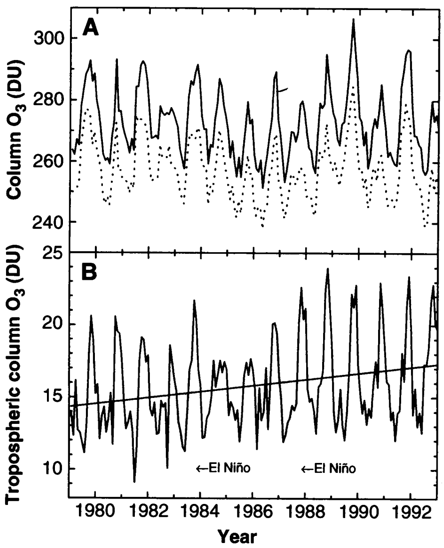

Fig. 2. (**A**) Averaged column O_3 over the mountain region (low O_3, dotted line) and over the nearby ocean (higher O_3, solid line). (**B**) Tropospheric column O_3 from sea level to 6 km is shown with a straight line as a linear least squares fit to the data. The slope of the line is 1.48 ± 0.40% per year. Two major El Niño events are indicated by shaded regions.

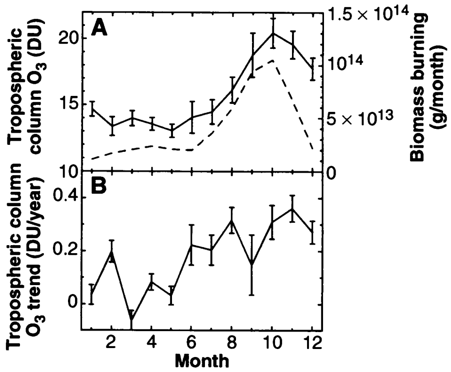

Fig. 3. (**A**) Climatological tropospheric O_3 (solid line) averaged from 1979 to 1992 (1 SD) and biomass burning (dashed line) in the latitude belt from 20° to 30°S (*17*). To convert from grams of biomass to grams of carbon, multiply by 0.5. (**B**) Tropospheric O_3 trends (DU per year) in each month from 1979 to 1992 (1 SD).

Niño years may be a result of a decrease in biomass burning during these wetter years (*18*).

An analysis of tropospheric O_3 trends from 1979 to 1992 for each month (Fig. 3B) supports this conclusion. The trends are higher, around 0.35 DU per year, between August and November versus about 0.15 DU per year at other times.

REFERENCES AND NOTES

1. J. A. Logan, M. J. Prather, S. C. Wofsy, M. B. McElroy, *J. Geophys. Res.* **86**, 7210 (1981).
2. W. Warmbt, *Z. Meteorol.* **29**, 24 (1979).
3. J. K. Angell and J. Korshover, *J. Climate Appl. Meteorol.* **22**, 1611 (1983).
4. J. A. Logan, *J. Geophys. Res.* **90**, 10463 (1985).
5. G. C. Tiao *et al.*, *ibid.* **91**, 13121 (1986).
6. J. Staehelin and W. Schmid, *Atmos. Environ.* **A25**, 1739 (1991).
7. D. W. Tarasick, D. I. Wardle, J. B. Kerr, J. J. Bellefleur, J. Davies, *Geophys. Res. Lett.* **22**, 409 (1995).
8. J. R. Herman, R. McPeters, R. Stolarski, D. Larko, R. Hudson, *J. Geophys. Res.* **96**, 17297 (1991).
9. A new retrieval algorithm for tropospheric column O_3 from radiances measured by TOMS has been developed by R. D. Hudson, J.-H. Kim, and A. M. Thompson [*J. Geophys. Res.* **100**, 11137 (1995)]. This technique has been applied only to the region bounded by 20°W and 60°E longitude and 20°S and 0°S latitude during the 1989 biomass burning season.
10. The choice is three adjacent longitudes (75.625°, 74.375°, 73.125°W) at 25.5°, 24.5°, 23.5°, and 22.5°S latitude for the column O_3 above the sea surface, and three adjacent longitudes (68.125°, 66.875°, 65.625°W) at 25.5°, 24.5°, 23.5°, and 22.5°S latitude for the column O_3 above mountains. There are a total of 24 data points in each monthly averaged TOMS data file in the respective regions we considered.
11. J. R. Herman, R. McPeters, D. Larko, *J. Geophys. Res.* **98**, 12783 (1993).
12. According to R. D. Hudson *et al.* (*9*), the TOMS algorithm is not very sensitive in detecting O_3 in the lower troposphere (about 60% efficiency in detecting O_3 in this layer). The a priori column O_3 between 1000 and 500 mb as in the TOMS algorithm is about 13 DU. Thus, if a value of 20 DU for the tropospheric O_3 is derived, this value must be corrected by the efficiency factor, about 60%, to get the right value (20 DU − 13 DU)/0.6 + 13 DU = 24.7 DU—giving a trend of 2.30 ± 0.62% per year relative to the initial value of 15.23 DU. In this report, the correction proposed above was not adopted.
13. J. Fishman, C. E. Watson, J. C. Larsen, J. A. Logan, *J. Geophys. Res.* **95**, 3599 (1990).
14. J. Fishman *et al.*, in *Fire in the Environment: The Ecological, Atmospheric, and Climatic Importance of Vegetation Fires*, P. J. Crutzen and J. G. Goldammer, Eds. (Wiley, New York, 1993), pp. 345–356.
15. V. W. J. H. Kirchhoff, A. W. Setzer, M. C. Pereira, *Geophys. Res. Lett.* **16**, 469 (1989).
16. V. W. J. H. Kirchhoff, R. A. Barnes, A. L. Torres, *J. Geophys. Res.* **96**, 10899 (1991).
17. W. Hao and M. Liu, *Global Biogeochem. Cycles* **8**, 495 (1994).
18. Other factors could contribute to the deviation of tropospheric O_3 from the linear trend during El Niño years, such as higher level clouds (due to deep convection) or less cloud in the lower troposphere, which would cause an underestimation of tropospheric O_3. Reflectivity and cloud height data can be examined in this region, but these analyses are beyond the scope of this report.

19. We thank R. S. Stolarski for sharing his insights into the TOMS data and M. Allen, W. M. Hao, A. Ingersoll, J.-H. Kim, R. Salawitch, S. Sander, J. Logan, H. B. Singh, M. O. Andreae, and two anonymous referees for valuable comments. We thank the Goddard Ozone Processing Team for use of their data before publication. Supported by NASA grant NAG1-1806 and National Science Foundation grant ATM 9526209 to the California Institute of Technology. Contribution 5644 from the Division of Geological and Planetary Sciences, California Institute of Technology.

25 January 1996; accepted 19 March 1996

Direct Measurement of Coupling Between Dendritic Spines and Shafts

Karel Svoboda, David W. Tank, Winfried Denk*

Characterization of the diffusional and electrotonic coupling of spines to the dendritic shaft is crucial to understanding neuronal integration and synaptic plasticity. Two-photon photobleaching and photorelease of fluorescein dextran were used to generate concentration gradients between spines and shafts in rat CA1 pyramidal neurons. Diffusional reequilibration was monitored with two-photon fluorescence imaging. The time course of reequilibration was exponential, with time constants in the range of 20 to 100 milliseconds, demonstrating chemical compartmentalization on such time scales. These values imply that electrical spine neck resistances are unlikely to exceed 150 megohms and more likely range from 4 to 50 megohms.

Dendritic spines are a prominent feature of neurons in the central nervous system, but their function is unknown (*1*). Speculation regarding the function of spines has centered on the diffusional and electrical resistance of the narrow neck that connects spines to dendritic shafts (*2–10*). Modeling studies suggest that synaptically induced Ca^{2+} concentrations in spines could reach micromolar values (*8, 9*) and thereby control biochemical processes central to synaptic plasticity (*10–12*). The spine head would thus function as a chemical compartment, isolating the concentration dynamics of intracellular messengers from the parent shaft and neighboring spines and providing, for example, the biophysical basis for homosynaptic specificity in long-term potentiation (*10, 12*). Spine necks have been hypothesized to influence synaptic strength (*2–4*), and spines have been proposed to act as discrete electrical compartments (*2, 3, 5*). For spine neck conductance comparable to synaptic conductance, the synaptic current depends on neck resistance, and changes in neck geometry could control synaptic weight (*3, 4*). The neck resistance might be too small to affect synaptic currents directly, but still large enough to increase synaptic potentials in the head, with respect to the shaft, sufficiently to limit the activation of voltage-controlled conductances to the spine head (*5*). A measurement of spine neck resistance is required to test these hypotheses.

Their small size (<1 μm) has prevented direct electrophysiological investigation of spines. Serial-section electron microscopy (SSEM) has provided information about spine geometry, which has been used to model the biophysical properties of spines (*5–9*). However, diffusional and electrical neck resistances are influenced by intracellular structures such as the spine neck apparatus (*5*) and are sensitive functions of neck geometry, which can be subject to distortion during the fixation process. Accumulations of Ca^{2+} can be localized to individual spines (*13–16*) and can, in fact, achieve micromolar concentrations (*17*). The spatiotemporal dynamics of intracellular free Ca^{2+} concentration ($[Ca^{2+}]_i$) are, however, markedly dependent on buffering and active extrusion (*18–20*), which are poorly characterized at the spine level—precluding an estimate of neck resistance from $[Ca^{2+}]_i$ measurements alone. The time course and spatial localization of changes in $[Ca^{2+}]_i$ might differ from those for other diffusible molecules. We have now measured the diffusional exchange between spine head and dendritic shaft with the use of fluorescence recovery after photobleaching (*21*) and fluorescence decay after photoactivation (*22*). The quantitative relation between diffusion and electrical conduction (*23*) then allowed us to estimate the spine neck conductance.

For the photobleaching experiments, CA1 neurons in rat hippocampal slices were filled with fluorescein dextran (FD) by whole-cell perfusion (*24*) and imaged with two-photon laser scanning microscopy (TPLSM) (Fig. 1A) (*25, 26*). Dendritic spines could be clearly resolved (Fig. 1B) as far as 150 μm below the slice surface. We used two-photon excitation to achieve (i) the necessary spatial confinement of bleaching or photoactivation, crucial for

Biological Computation Research Department, Bell Laboratories, Lucent Technologies, 600 Mountain Avenue, Murray Hill, NJ 07974, USA.

*To whom correspondence should be addressed. E-mail: denk@bell-labs.com.